Sensors and Actuators B 188 (2013) 857–866

Contents lists available at ScienceDirect

Sensors and Actuators B: Chemical

journal homepage: www.elsevier.com/locate/snb

An investigation into relative humidity measurement using an aluminosilicate sol–gel thin film as the active layer in an integrated optical Bragg grating refractometer☆

Dominic J. Wales[a,b,*], Richard M. Parker[a,b], James C. Gates[a], Martin C. Grossel[b], Peter G.R. Smith[a]

[a] Optoelectronics Research Centre, Faculty of Physical Sciences and Engineering, University of Southampton, Southampton SO17 1BJ, United Kingdom
[b] Department of Chemistry, Faculty of Natural and Environmental Sciences, University of Southampton, Southampton SO17 1BJ, United Kingdom

ARTICLE INFO

Article history:
Received 5 March 2013
Received in revised form 12 July 2013
Accepted 24 July 2013
Available online xxx

Keywords:
Bragg grating
Refractive index sensor
Relative humidity
Integrated optics
Sol–gel

ABSTRACT

We have demonstrated that a planar integrated optical Bragg grating sensor chip, fabricated using a direct UV-writing approach, can perform as an all-optically accessed relative humidity sensor. Using a simple mesoporous silica thin film enabled operation across the range 0–100%RH, however a thickness decrease of 25% caused by hydrolytic degradation of the silica thin film resulted in a permanent decrease in sensitivity after 1–2 weeks use. Grafting the thin-film with aluminium oxide is shown here to prevent hydrolytic degradation with long-term sensitivity maintained. Aluminium oxide grafting offers the additional benefit of enhanced sensitivity, up to 3.5 times that of the silica analogue; the sensitivity of the aluminium oxide modified thin film device = 0.69 ± 0.05%RH/pm, in the range 0–60%RH within a gas flow system, whilst the sensitivity of the silica thin film sensor device = 2.47 ± 0.18%RH/pm. Long-term measurements, in static ambient lab conditions, were in excellent agreement with a commercial humidity sensor and also indicated that the thermal compensation afforded by the on-chip reference gratings was sufficient to prevent any drift in calibration. As with all humidity sensors, contamination of the sensor occurred. But for the aluminium oxide device, this was easily removed by rinsing with common organic solvents and the sensitivity was repeatedly and reproducibly restored. The device is accessed using optical fibre technology and is intrinsically safe in flammable environments.

1. Introduction

Humidity impacts on a diverse range of industrial, agricultural, medical and domestic processes, including chemical gas purification, soil moisture monitoring, incubation processes, and intelligent fine control of ambient environments within buildings [1]. In situations such as industrial manufacturing plants, it can be essential that any measuring techniques be intrinsically spark-free [2].

The humidity of a system is typically quoted in terms of relative humidity, %RH, and is defined as the ratio of the actual vapour pressure of water vapour to the saturation vapour pressure of water over a plane liquid water surface at a given temperature and is expressed as a percentage [3].

The earliest recorded attempt at humidity sensing was by Hooke using an 'oat beard hygrometer' [4]. Early humidity measuring techniques including twisted hair hygrometers, wet and dry bulb psychrometers (including the variants, the sling psychrometer and the Assmann ventilated psychrometer) and chilled mirror hygrometers [5], all have largely been superseded by electronic methods. The main disadvantage with these mechanical devices is that the techniques employed do not lend themselves to facile miniaturisation or remote and distributed sensing. To overcome these disadvantages miniaturised electrical humidity sensors were developed, with ~75% of commercially available systems now capacitive electrical hygrometers [6]. These miniaturised electrical devices transduce the moisture uptake in ceramic thin films into a change in capacitance. While ceramic-based devices possess very high sensitivities, they require sporadic heating to remove condensed water to maintain their sensitivity [6]. To overcome this issue, sensor devices with 'on-device' heating elements have been reported [6], however these active components increase power consumption and introduce a spark risk in flammable environments. Less common resistance-based electrical hygrometers transduce humidity into changes in impedance within a ceramic, organic polymer or electrolyte doped material [6]. However,

* Corresponding author at: Department of Chemistry, Faculty of Natural and Environmental Sciences, University of Southampton, Southampton SO17 1BJ, United Kingdom. Tel.: +44 2380596769.
E-mail address: dw405@soton.ac.uk (D.J. Wales).

0925-4005/$ – see front matter © 2013 The Authors. Published by Elsevier B.V. All rights reserved.
http://dx.doi.org/10.1016/j.snb.2013.07.089

miniaturised resistivity transducer devices suffer from degradation of the organic polymer in both high humidity and temperatures [6], while electrolyte-doped materials need regular maintenance to maintain a stable response [4]. Further, the use of ceramic materials similarly requires on-chip heating elements, again with the additional spark-risk beyond that which is intrinsic to all electrical based sensors.

In contrast, optical fibre sensors are intrinsically suitable for use in hazardous or explosive environments. There are many examples in the literature of optical fibre relative humidity sensors [7]. Krishnaswamy et al. have reported optical fibre long-period Bragg grating relative humidity sensors [8,9] of which the latest iteration is a nanofilm-coated photonic crystal optical fibre containing long-period gratings [10]. This device exhibits a sensitivity of 7.0×10^{-4}% change in RH for a 1 pm wavelength change within its most sensitive operating range (22–29%RH). However, the operable temperature of the sensor is limited by the thermal stability of the organic components of the nanofilm coating; as poly(acrylic acid) begins to thermally degrade in the temperature range of 70–140 °C [11].

Integrated optical hygrometers are also largely suitable for use in hazardous or explosive environments as well as affording the ability to interrogate remotely large multi-sensor arrays via optical fibre [12]. In addition, integrated optics allows for on-chip thermal compensation [13] and the combination of multiple optical functions in a single device, allowing for multi-parameter analysis [14]. While there exists potential for planar integrated optical hygrometers to be applied to the monitoring of humidity within hazardous environments, an important role may also be as part of a diagnostic tool to prevent moisture damage to photonic integrated circuits (PICs), where the stability of the packaging and UV-curable epoxy adhesives used to manufacture PICs in optical network systems can be severely impacted in high humidity environments [15].

There are relatively few examples of planar integrated optical hygrometers reported in the literature. Skrdla et al. presented a planar waveguide water vapour sensor that utilised an organic dye encapsulated in a sol–gel thin film. While this demonstrated a sensitivity range of 1–70%RH with a response time of <1 min, the restricted interrogation wavelength of 514.5 nm is incompatible with standard telecoms equipment that typically operate at near-infrared wavelengths [16]. In addition these devices have the potential disadvantage of photobleaching [17]. Bhola et al. reported an optical micro-ring resonator hygrometer with a sensitivity of 16 pm/%RH in the range 0–72%RH and a response time of ~200 ms, although highly sensitive the device has the drawback that the temperature of the device needs to be kept constant to within ±0.1 °C to achieve an accuracy of ±0.5%RH [18]. Prosposito et al. have recently reported preliminary studies of a potential hygrometer consisting of a sol–gel waveguide containing a Bragg grating on a planar substrate [19], but it was only applied to the detection of liquid water and not relative humidity. More recently Rosenberger et al. have reported a planar integrated Bragg grating device fabricated from bulk poly(methyl methacrylate) and this device was demonstrated as a relative humidity sensor [20]. However, a key potential issue of this device is the susceptibility of poly(methyl methacrylate) to swelling and catastrophic fracturing in the presence of solvent vapours [21]. In contrast the planar integrated Bragg grating sensor devices of the type demonstrated herein allow for on-chip temperature compensation [8,22] and are resistant to a wide range of common solvents [23].

2. Background

A Bragg grating is a periodic modulation of refractive index along a waveguiding channel, which in reflection acts as a wavelength-selective mirror. Bragg gratings are inherently sensitive to both temperature and strain, however if the light within the waveguide is able to interact with the ambient environment, then evanescent coupling allows for a change in the optical characteristics which can be sensed [24]. Changes in this environment alter the effective refractive index, n_{eff} of the Bragg grating and correspondingly the shift in the Bragg wavelength (λ_B). This is shown schematically in Fig. 1(a).

By incorporating several Bragg gratings within a single waveguide and interrogating the wavelength shift of the reflected Bragg peaks at near infrared wavelengths, an integrated optical refractometer can be produced (Fig. 1(b)). Such waveguides can be fabricated directly with a UV-laser into a planar photosensitised silica-on-silicon substrate to produce a wide range of integrated optical devices, such as optical splitters and Mach–Zehnder interferometers [25,26]. The expansion of this approach, through the controlled modulation of a pair of interfering UV-laser beams [27,28], allows for the simultaneous definition of Bragg gratings within these waveguides without the need for additional photolithographic processing. The high spectral fidelity of the Gaussian-apodised grating fabricated by this method allows the Bragg wavelength to be determined with sub-picometre precision, corresponding to changes in the refractive index of the analyte down to 10^{-6}. A thorough review on the fabrication of planar integrated Bragg gratings devices using the direct UV-writing approach is given by Sparrow et al. [29].

Exposed integrated optical Bragg gratings have previously been shown to be sensitive to the formation of physisorbed water on the surface of the exposed waveguide [30]. When a layer of physisorbed water condenses onto the surface, air of refractive index 1.00 is replaced by a film of water of index 1.33, raising the average refractive index (n_{eff}) experienced by the optical mode of the waveguide. The Bragg grating can be used to probe this increase in n_{eff} through the corresponding increase in the Bragg wavelength. While this device was able to probe the phase change of water on the surface at the dew point; for a practical optical hygrometer it will be necessary for the Bragg grating sensor to operate at far lower humidity levels, where the physisorbed water layer would be only a few nanometres thick. In such a situation, only a very small fraction of the evanescent field would be exposed to the change in refractive index upon changes in the thickness of this thin film of moisture, corresponding to a small Bragg wavelength shift upon humidity change. Here we propose that to increase the sensitivity of such a Bragg grating device, an increase in the sensing surface area is required to amplify the effect of the formation of such water layers.

One approach to increase the surface area of the sensor exposed to water vapour is through the use of a porous matrix deposited on top of the waveguide. Many different porous materials able to incorporate guests are reported in the literature as sensing elements; from metal-organic frameworks [31] and zeolites [32] to polymer hydrogels [33] and silica sol–gels [34]. However, miniaturised electrical humidity sensors based on metal-organic frameworks or zeolite transducers, are generally operated at temperatures above 120 °C, which requires additional power and may present an ignition risk in flammable environments [26], whilst organic polymer hydrogels can be chemically and thermally unstable in harsh operating conditions [26]. In contrast, sensor transducer elements fabricated from silica sol–gels offer improved physical rigidity and thermal stability [35], important when monitoring refractive index. In addition, for preferential physisorption of water to occur, a hydrophilic surface is desired.

Mesoporous sol–gel films have been previously reported for application in the sensing of vapours [36,37]. These metal oxide thin films (typically silica) can be fabricated at low temperature and in mild conditions, with fine control of the porous mesostructure [38]. The hydrophilic silanol-coated pores, combined with the

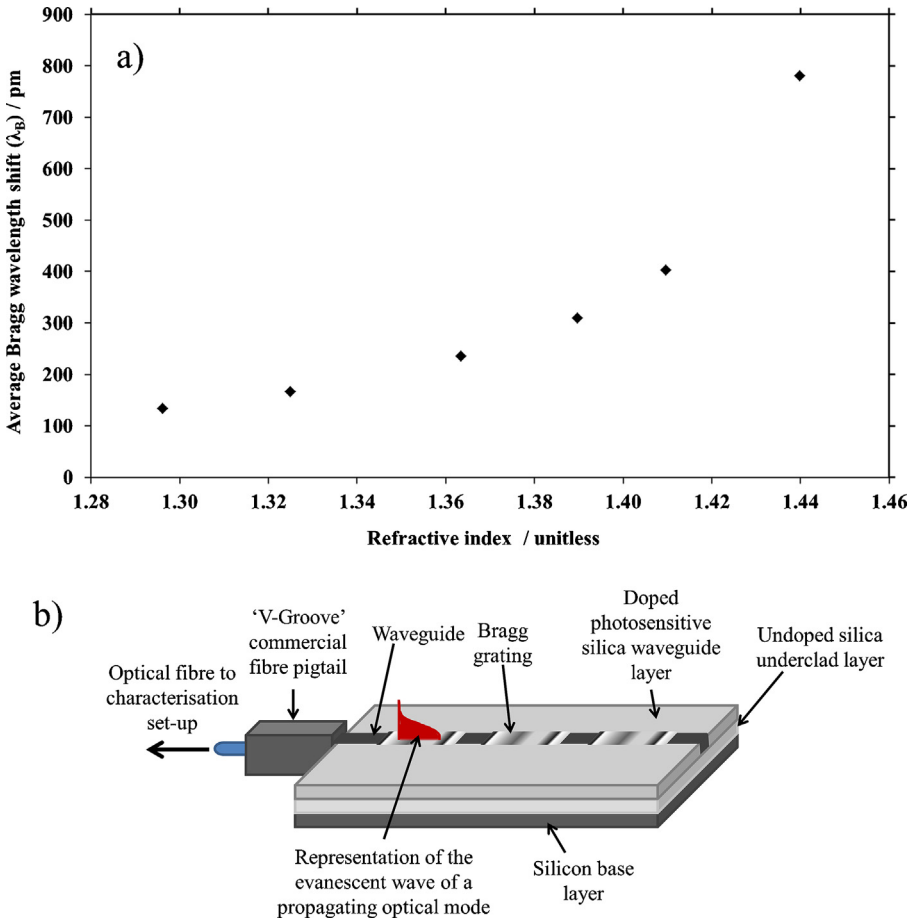

Fig. 1. (a) Calibration curve of a Bragg grating refractometer device to changes in refractive index and (b) an illustration of the Bragg grating refractometer devices used within this work.

large surface area available for adsorption of water molecules lend silica sol–gel thin films to application in humidity sensing.

Here we investigate the long-term stability of silica sol–gel for use in optical hygrometers and explore the advantages of introducing an alumina-grafted surface into such systems. We report an integrated optical Bragg grating hygrometer fabricated by the direct UV-writing of Bragg gratings into a silica-on-silicon substrate combined with a mesoporous sol–gel thin film as the sensing element, without the need for photolithographic or clean-room processing. The sensor is capable of monitoring relative humidity from 0 to 100%RH, with a standard error of ±0.3%RH measurable linearly across the range 0–60%RH; this covers the operating range for processes such as textile processing, pharmaceutical manufacture and storage [39].

3. Experimental

3.1. Integrated optical Bragg grating refractometer

Flame hydrolysis deposition was used to deposit a fully dense, glassy germanium-doped silica layer onto a thick thermal oxide (~17 μm) coated silicon wafer (~1 mm). Into this doped core layer, channel waveguides containing Bragg gratings were written using a pair of interfering UV-laser beams (λ = 244 nm). A process known as direct UV grating writing allows for the simultaneous formation of both waveguides and, through modulation of the laser intensity, Bragg gratings [8,9]. The UV-written waveguide dimensions were defined by the thickness of the planar core layer and the width of the UV beam, both approximately 5 μm. Multiple Bragg gratings were written into a single waveguiding channel, each Bragg grating being 2 mm long and with a period between 525 and 542 nm, satisfying the Bragg condition to reflect at wavelengths between 1520 and 1570 nm.

A commercial optical fibre 'pigtail' was aligned and robustly attached to the integrated Bragg grating device via a commercially available 'v-groove' optical fibre assembly and UV-cured adhesive. Solubilisation of the UV-cured adhesive by water vapour was not expected; the UV-cured adhesive is very insoluble in water. Regardless, the 'pigtail' joint was routinely protected by a polymer sheath, which did not interfere with operation of the sensor, and acted to prevent/lessen the degradation of the UV-cured adhesive due to ingression of solvent vapour during the solvent washing/steps to regenerate the sol–gel thin film. The reflectance spectrum of the device was interrogated through the optical fibre pigtail by an infrared erbium fibre amplified stimulated emission (ASE) source (1520–1570 nm) and was analysed by an optical signal analyser (OSA) connected via an optical circulator. The central wavelength of the Bragg peak was calculated from a Gaussian fit, allowing for sub-picometre resolution. The effective refractive index, n_{eff} is presented in this work as a shift relative to an initial value, Δn_{eff}, rather than as an absolute refractive index.

3.2. Mesoporous sol–gel thin films

Commercially available compounds and solvents were obtained from Sigma–Aldrich, Fisher Scientific and Acros Organics and used as supplied without further purification, unless noted. AcroSeal® grade tetraethoxysilane (TEOS) was used in sol–gel preparation.

De-ionised water (>18.1 MΩ) was used in the fabrication of the mesoporous thin film and for all humidity sensing experiments. Ethanol was distilled over calcium sulphate and used immediately. Cetyltrimethylammonium bromide (CTAB) was dried and stored in a desiccator in vacuo before use. Dry nitrogen gas refers to Oxygen Free Nitrogen (OFN), 99.9% purity.

Surface profile data (step height and surface roughness, R_a) was recorded using a KLA *Tencor P.16* surface profiler connected to a PC running Profiler v7.21 software. Spin coating was performed using a Speciality Coating Systems Inc. *G3P-8 Spincoat*. Energy-dispersive X-ray (EDX) spectra were collected using an Oxford Instruments *INCA* X-ray detector attachment (Be window, connected to a PC running *INCA* EDX software) on a *Zeiss Evo 50* scanning electron microscope in high vacuum mode (20 μm aperture), accelerating voltage = 20 kV, gun current ~2.41 A, working distance = 9.5 cm and magnification ~×5000, controlled by a PC running Zeiss Smart SEM software. The samples were coated with 77 nm of carbon before analysis.

The mesoporous silica sol–gel thin films were fabricated using a modified procedure utilising the evaporation-induced self-assembly (EISA) technique [40] which is summarised as follows: Tetraethoxysilane (TEOS, 10 mL, 4.48×10^{-2} mol) was added to distilled ethanol (7.9 mL, 1.34×10^{-1} mol), de-ionised water (6.4 mL, 3.58×10^{-1} mol, resistivity > 18.1 MΩ) and aqueous hydrochloric acid solution (0.1 M, 22.4 μL) and allowed to hydrolyse for 90 min at 60 °C under an inert atmosphere. After cooling to room temperature, the concentration of hydrochloric acid within the reaction mixture was increased to 7.3×10^{-4} mol dm^{-3} by the addition of 1.0 mL of aqueous hydrochloric acid solution (0.2 M). The sol was stirred for 15 min under nitrogen and then 'aged' without stirring at 60 °C in air for a further 15 min. Finally, distilled ethanol (75 mL) and the pore template, cetyltrimethylammonium bromide (CTAB, 2.55 g, 7.00×10^{-3} mol) were added with rigorous stirring to afford a colourless, slightly turbid sol. The concentration of CTAB in the final sol (7.0×10^{-2} mol dm^{-3}) was chosen so that the desired worm-like porous mesostructure would be formed upon spin deposition and subsequent calcination [41].

Before application of the mesoporous thin films onto the surface of the waveguide layer, the device was cleaned with "piranha" solution (98% H_2SO_4:30% H_2O_2, 3:1) for 45 min, washed copiously with de-ionised water and then dried thoroughly under a flow of nitrogen. Immediately following cleaning, the sol was applied to the sensor device by spin deposition of 0.2 mL of the sol solution at 2000 rpm for 1 min. The deposited layer was calcined at 400 °C for 1 h (heating rate 1.5 °C/min) in a N_2/O_2/Ar (~2.1:~0.7:~0.5 L/min) atmosphere to form the mesoporous thin film. The average thickness of this silica sol–gel mesoporous thin film was found to be 230 ± 27 nm by step profilometry; the large associated errors are attributed to the significant topographical waviness measured in all spin coated samples of the viscous sol.

Aluminium oxide was grafted into the mesoporous silica film using a modification of a literature procedure [42], whereby an aqueous solution of 'aluminium hydroxide/oxide' species was formed by the dissolution of anhydrous aluminium chloride (~1.6 g) in de-ionised water (25 mL). The silica mesoporous thin film was immersed in this solution at 80 °C for 6 h, rinsed copiously with de-ionised water and dried under a stream of nitrogen gas. The substrate was then calcined at 450 °C for 3 h (heating rate 1.0 °C/min) in a N_2/O_2/Ar (~2.1:~0.7:~0.5 L/min) atmosphere to consolidate the aluminium oxide. Mesoporous silica is known to slowly dissolve under these reaction conditions until the protective alumina layer is fully formed. To compensate for this erosion, a silica mesoporous thin film of ~300 nm was initially prepared by deposition at a lower spin speed. This film subsequently reduced in thickness during the reaction to 260 ± 24 nm for the aluminium oxide grafted mesoporous thin film. In this way both aluminosilicate and silica films of comparable thickness could be fabricated allowing for direct comparison.

The presence of aluminium oxide was confirmed by the appearance of a weak intensity peak on the EDX spectrum that corresponded to the aluminium K_α emission (1.486 keV) adjacent to a higher intensity and broader peak corresponding to the silicon K_α emission (1.739 keV). It should be noted that this experiment was carried out on a separate device to that used for humidity sensing experiments as the conductive layer of carbon used to prevent surface charging in the scanning electron microscope would have irreparably contaminated the sensing layer. However, as the grafting procedure was identical for both samples, it was inferred that aluminium oxide grafting was achieved in the case of the sensor device.

3.3. Optical hygrometry

The gas delivery apparatus for optical hygrometry experiments is shown schematically in Fig. 2. The integrated optical Bragg grating device ('BGD') was mounted within a flow cell and interrogated whilst exposed to a flow of nitrogen gas. The temperature within this cell was monitored via a thermocouple.

The water vapour in the nitrogen carrier gas was introduced by bubbling dry nitrogen gas (typically ~3.5 L/min) through a reservoir of de-ionised water ('H_2O') and by altering the water temperature the water vapour concentration was controlled. The temperature of the reservoir was incrementally changed using an external water bath, the temperature of which was raised or lowered with either a hotplate or addition of ice, respectively. To return the integrated Bragg grating hygrometer device to its initial state after exposure to water vapour, the reservoir was bypassed allowing the cell to be purged with dry nitrogen gas (>5 L/min). In addition, before a humidity measurement was recorded, a stable %RH value for the moist nitrogen gas flow was first achieved by altering the water bath temperature and referenced against an in-line electronic commercial *Testo 625* hygrometer ('%RH'). Once a constant %RH value was achieved, the moist nitrogen gas was introduced into the cell containing 'BGD'. It should be noted that while the vapour flow was stabilising, the sensor device was kept under a secondary dry nitrogen flow to avoid contamination.

The full spectrum of the reflected peaks of the Bragg gratings was sampled every 20–25 s via the OSA. The average shift in Bragg wavelengths upon exposure of the sensor device to changes in humidity were calculated by subtraction of an average over at least 5 min of the Bragg wavelength measured during the exposure to water vapour from the average of the stable background, measured under dry nitrogen before and after, allowing thermal effects to be minimised.

4. Results and discussion

4.1. Integrated optical Bragg grating hygrometer

A channel waveguide containing eight Bragg gratings was fabricated (Fig. 3(a)). Each Bragg grating acted as an independent refractometer, capable of detecting changes in the refractive index near the surface through the corresponding shift in the Bragg wavelength. This sensor surface was partially coated with a mesoporous, transparent and crack-free silica sol–gel thin film, ~250 nm thick. The mesoporous nature of the thin film was achieved by doping the silica sol with a surfactant, CTAB via the evaporation induced self-assembly (EISA) technique [35]. By only covering the central four Bragg gratings underneath the sol–gel, the two peripheral Bragg gratings on either side could be used for self-referencing against other environmental fluctuations; primarily temperature. The

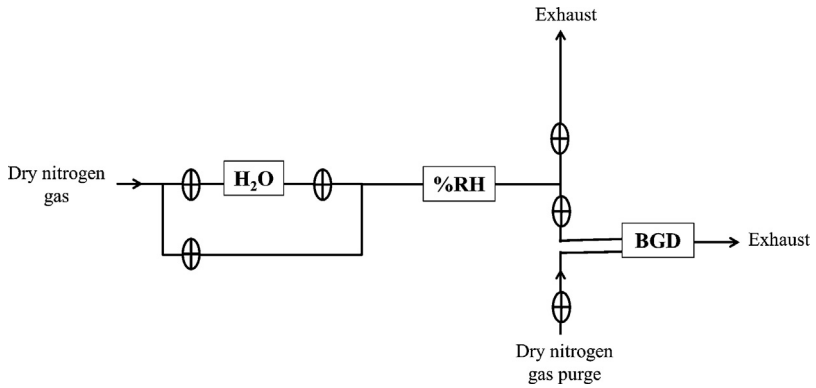

Fig. 2. A schematic of the gas flow network used to investigate the Bragg grating response to changes in humidity. Water vapour was generated by bubbling dry nitrogen gas through a de-ionised water reservoir ('H_2O'). '%RH' represents the electronic reference hygrometer and 'BGD' is the location of the flow cell containing the integrated optical Bragg grating device. A second nitrogen purge was used to maintain a dry atmosphere between measurements.

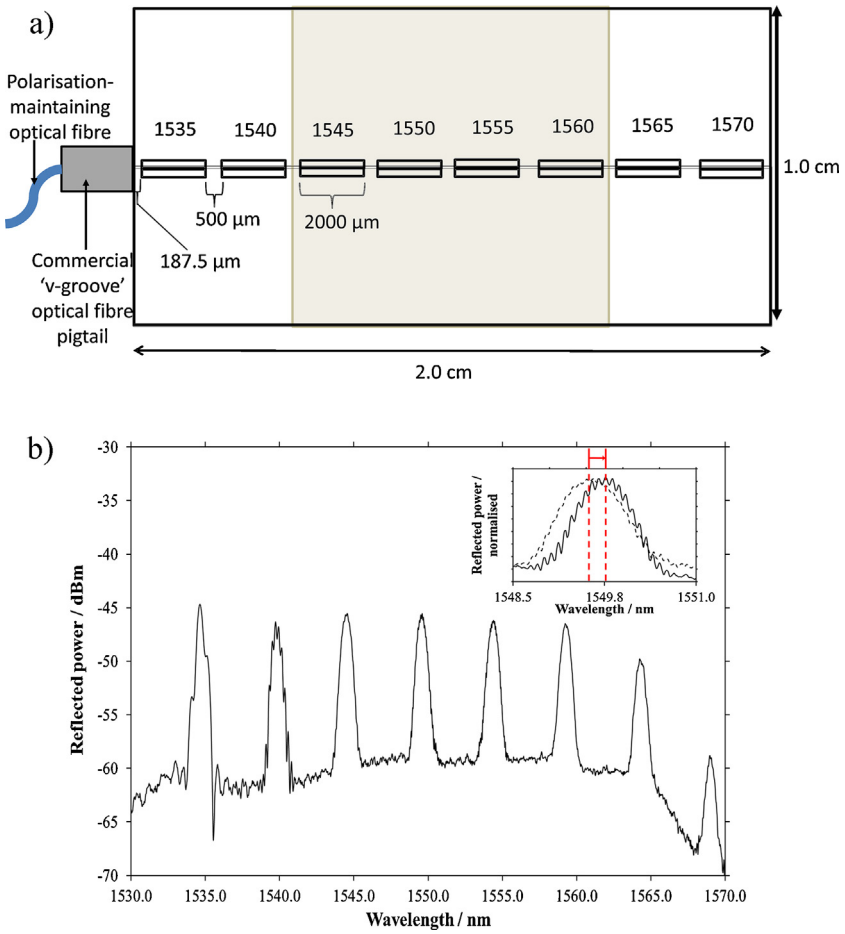

Fig. 3. (a) A schematic of the planar integrated Bragg grating hygrometer, illustrating the location of the eight Bragg gratings along the waveguide and their approximate Bragg wavelength in nm. The grey region designates the mesoporous thin film. The readout system is connected to the chip using an optical fibre and is robustly pigtailed using standard telecomm assembly techniques. (b) The reflected Bragg grating spectrum of the bare device as collected from the optical spectrum analyser (OSA) and (inset) highlighting the shift in Bragg wavelength of a Bragg grating after coating with the alumina-grafted thin film (solid black) relative to the same Bragg grating in the bare state (dashed black).

corresponding Bragg peak for each of the eight Bragg gratings is shown in Fig. 3(b); this spectrum was collected with the bare device, i.e. no sol–gel thin film on the device. It should be noted that the Bragg gratings at the extremities of the device, while suitable for temperature referencing, exhibited spectral fringes which degraded the quality of fitting. As such, these gratings (1535 and 1570 nm) were not used explicitly for referencing in the following work, but did allow for further confirmation of thermal trends that were observed (Fig. 3(b)).

The Bragg grating sensor was exposed to nitrogen gas containing a controlled concentration of water vapour and interrogated optically in the infrared region. The measurements were taken by cycling between dry nitrogen (recorded at 0%RH) and the vapour loaded flow to give a reference value and this protocol was adopted

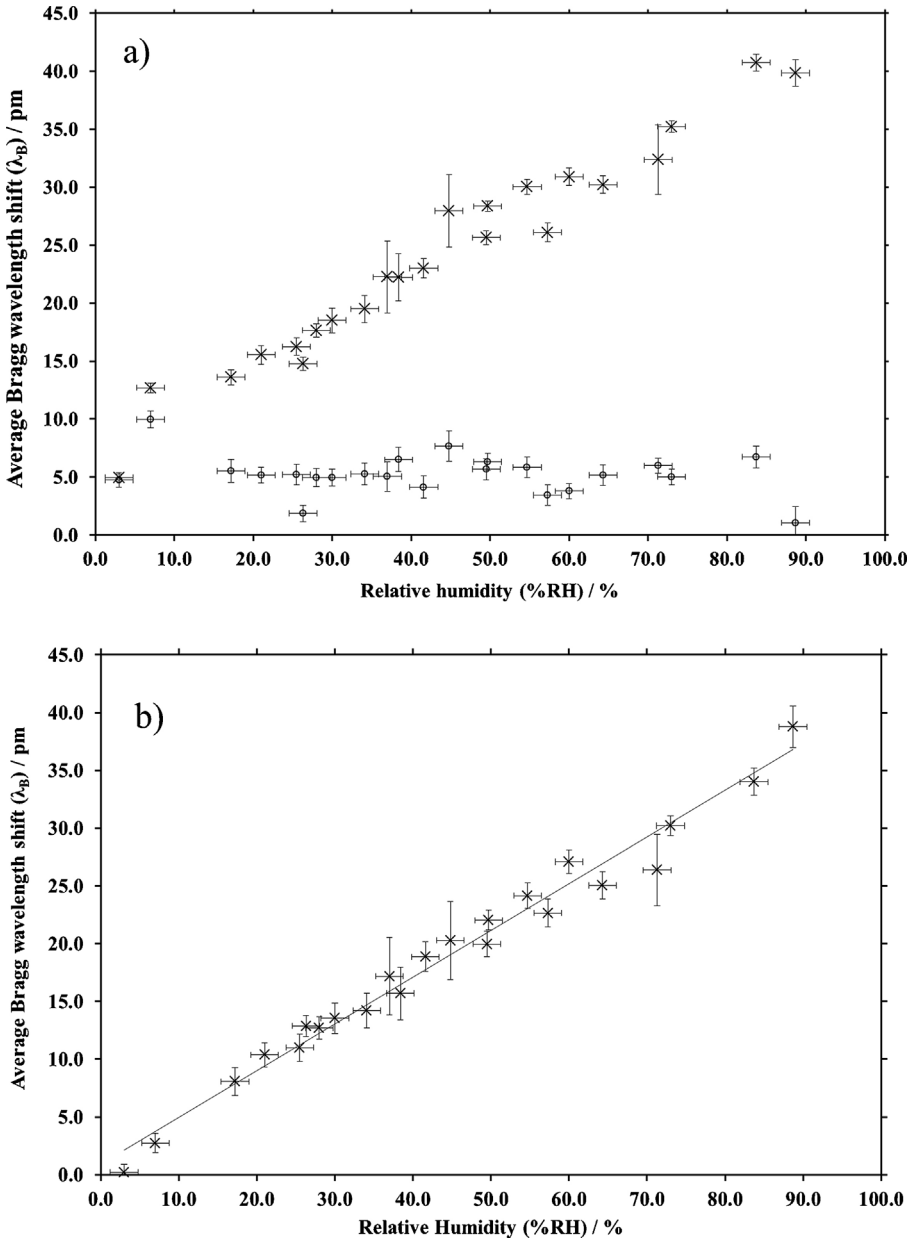

Fig. 4. (a) The average Bragg wavelength shift of the mesoporous silica sol–gel thin film region (crosses) increases when exposed to increasing relative humidity, %RH. In contrast the two uncovered Bragg gratings (circles) show no response to humidity change. (b) After subtraction of reference gratings an improved linear response to increasing relative humidity was observed, demonstrating on-chip thermal compensation.

for all measurements within the flow-cell system. By comparing the observed Bragg wavelength shift with the relative humidity recorded by an electronic hygrometer located in close proximity, the sensitivity of the device to changes in humidity could be probed. As shown in Fig. 4(a), it was found that there was a linear response between the average Bragg wavelength shift recorded by the sol–gel covered region upon increasing the relative humidity from 3%RH to 90%RH. In contrast, the Bragg wavelength shift measured for the uncovered Bragg gratings was ~5 pm for all values of relative humidity above 3%RH. This independence between Bragg wavelength shift and humidity is attributed to a rapid saturation of the surface with water, with further subtle variations in the average Bragg wavelength shift primarily due to changes in temperature during the experiment. Temperature referencing was achieved by a first-order subtraction of the average Bragg wavelength shift for the uncovered region from the average Bragg wavelength shift of the covered region. This temperature referencing method is based on a good first approximation that the average $\delta n/\delta T$ that the optical mode experiences, where n is the refractive index, in the region covered with the ~250 nm thickness thin film is comparable to that of the uncovered region. Thus changes in temperature should affect all gratings equally and so full compensation for such fluctuations was achieved passively and on-chip [19]. After applying on-chip referencing, the linearity of the average Bragg wavelength shift with increasing humidity was found to be improved, with the linear regression coefficient of determination (R^2) increasing from 0.96 to 0.98 (Fig. 4(b)). In all figures, unless explicitly stated, the x-axis error bars represent the average associated uncertainty of an average %RH value calculated from a range of %RH values measured with the *Testo 625* relative humidity sensor, which is quoted as having an accuracy of ±2.5%RH [43]. The y-axis error bars represent the associated average uncertainty of an average Bragg wavelength shift calculated for either the uncovered or covered Bragg gratings at a particular %RH value.

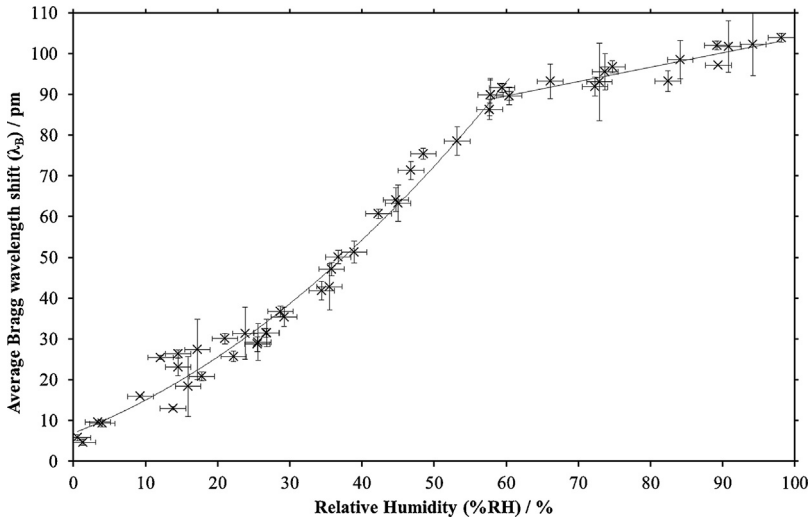

Fig. 5. Three data sets were collected from 0–100%RH after prolonged exposure to elevated humidity (>95%RH). Lines are guides for the eye only.

This result demonstrates that the refractive index change upon physisorption of water into the pores of a silica sol–gel is sufficient to be detected by the high precision Bragg gratings reported here. The device exhibited a linear response to relative humidity within the broad operating range of 3–90%RH, with sensitivity to a single percentage change in %RH being achievable. The majority of relative humidity measurement applications fall within this range and with further optimisation of the film thickness and enhancement of the evanescent modal overlap we believe that this technique can match the state-of-the-art [44] with the additional real-world benefits of multiplexed sensing and self-referencing demonstrated here.

4.2. Studies into long-term stability – aluminosilicate sol–gels

The shortcoming of all silica based sol–gel films in the field of hygrometry is their inherent solubility in water, leading to hydrolytic degradation. After 2–3 days of continued experimentation at elevated humidity (often exceeding 90%RH) and ~11 days in ambient atmosphere (typically 45%RH), a 50% decrease in the sensitivity of the device was observed. It was initially proposed that this decrease in sensitivity was due to a reduction in the active sensing surface area caused by retention of moisture within the pores of the sol–gel. To test this, the device was heated in air at 50 °C for 24 h however the device was not restored to its original state. A higher drying temperature was not used as this could have caused thermal degradation of the optical glue used to attach the optical fibre. It should be noted that both the sol–gel thin film and the Bragg grating sensor chip would not have been degraded by a higher drying temperature; the sol–gel thin film is calcined on the sensor chip up to 450 °C and no degradation was observed after this treatment. Furthermore, the storage of the device in vacuo over desiccant for 24 h also did not improve the sensitivity.

Surface profilometry of the device revealed that the sol–gel film had decreased by ~25% relative to its original thickness. It is proposed that this loss of film thickness is due to collapse thereby reducing the active surface area for water physisorption, leading to the loss of sensitivity. Indeed, it has been previously reported [45] that the thickness of silica sol–gel thin films decreases after fabrication until a stable thickness is reached, due to exposure to ambient humidity. Rapid thickness decreases have also been demonstrated to occur when mesoporous silica sol–gel thin films were fully immersed in aqueous solution [37] due to hydrolytic degradation. Prevention of this degradation of silica sol–gels has been reported [37] by treatment of the mesoporous thin films with aluminium oxide either during synthesis or through a post-fabrication treatment [37]. In this work, a post-fabrication treatment was applied as this does not alter the structure of the already formed mesoporous network within the thin film [46] allowing for direct comparison between the silica and the treated analogue.

A Bragg grating hygrometer was prepared identically to the previously discussed silica system with the addition of post-fabrication grafting of aluminium oxide as discussed above. After the aluminium oxide grafting treatment, the thin film was found to have remained transparent and crack-free. Optical hygrometry with on-chip temperature compensation was repeated with this new device as per the silica thin film device. While the behaviour of the uncovered reference gratings was unchanged, it was found that the sensitivity to changes in humidity for the covered gratings had more than doubled and that the profile was no longer found to be linear, but instead exhibited a more complex relationship between relative humidity and the average Bragg wavelength shift (Fig. 5).

The increase in sensitivity is attributed to the aluminosilicate mesoporous thin film having a higher refractive index compared to the silica mesoporous thin film. The higher refractive index of the aluminosilicate mesoporous thin film 'pulls' the optical mode further out of the waveguide core. Thus, more of the power within the evanescent wave interacts with the sol–gel sensor layer. The higher refractive index was confirmed by monitoring the Bragg wavelength shift caused by deposition of the silica layer and comparing this to the Bragg wavelength shift during the fabrication of the aluminosilicate mesoporous thin film on the device (Fig. 3(b) (inset)) with the final Bragg wavelength shift after fabrication of the aluminosilicate mesoporous thin film determined to be ~370 pm, whilst the final Bragg wavelength shift after deposition of a silica mesoporous thin film was ~270 pm. It is known that the larger the change in refractive index, the larger the Bragg wavelength shift. Furthermore, both layers were of equivalent thickness within error, therefore confirming that the refractive index of the aluminosilicate thin film was greater than the silica thin film.

The response time of the device in a flow system was determined by taking an average of three independent sensing events, where the humidity was stepped from 0%RH to 90%RH and the time taken for a stable Bragg wavelength shift to be achieved was recorded. The response time of a gas sensor is defined as the time taken to achieve 90% of the final change after a step increase of the concentration of the analyte gas [47]. For this sensor, 90% of the final

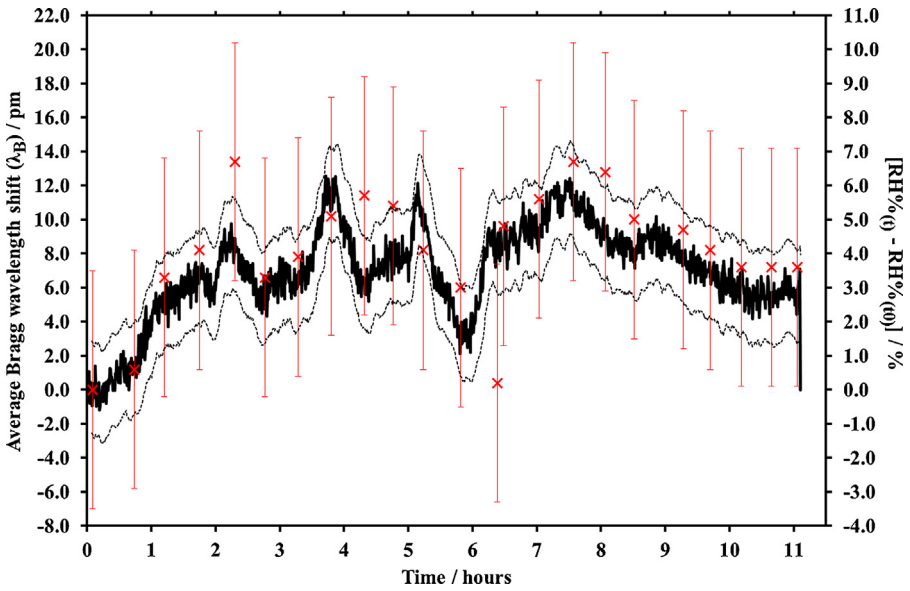

Fig. 6. The close agreement between the Bragg wavelength shift of the aluminosilicate-coated optical Bragg grating hygrometer (black line) with the commercial electronic hygrometer (red crosses) relative to the initial value, when both devices were exposed to the open laboratory for 11 h. The range of the associated error of the Bragg grating humidity sensor is given between the two dashed black lines. The accuracy of each measurement using the electronic hygrometer is shown by the red vertical error bars. (For interpretation of the references to colour in this figure legend, the reader is referred to the web version of this article.)

constant Bragg wavelength value was reached in 55 s. A 90% shift is sufficient to differentiate between all %RH values; an identical response curve would be generated, but just at Bragg wavelength shift values 10% lower than in Fig. 5. Therefore the viable response time of the humidity sensor device is <1 min.

The stability of the aluminosilicate-modified device was tested through exposure to >95%RH for ~2 h followed by three repeat measurements of the complete sensitivity profile from 0%RH to 100%RH. In all three cases, it was found that the sensor responses of the device at all relative humidity values were in excellent agreement with each other, demonstrating the much improved stability of the aluminosilicate-grafted surface (Fig. 5). This stability to hydrolytic degradation was further confirmed though surface profilometry with the thickness of the mesoporous layer found to be unchanged throughout these experiments.

The non-linear sensitivity response of the Bragg refractometer to relative humidity when grafted with aluminosilicate enabled even greater sensitivity at humidity ranges of interest for real-world applications. In the region of 0–60%RH, the aluminium oxide grafted device exhibited sensitivity up to 3 times greater than exhibited by the analogous silica device. Performing a linear regression to the data in the range 0–60%RH and using the standard error of the Bragg wavelength shift, a calculation of the precision of the aluminosilicate modified thin film device at room temperature yielded a value of ±0.3%RH. From Kaye and Laby [48], at 4 °C, the absolute concentration of water in air drops by a factor of three from its room temperature value (~21 °C) so the precision of the device is expected to worsen to ±0.9%RH. Above ~60%RH there is a reduction in sensitivity exhibited by the aluminosilicate device which is shown as the shallower gradient on the plot; this was demonstrated in all three data sets. This limits operation at high water concentrations and thus would limit operation at higher temperatures; however it would be relatively simple to make a less sensitive device by reducing the porosity of the active sensing sol–gel thin film. It is proposed that at relative humidity values <60%RH the response of the device follows a similar trend as evident in Fig. 1(a). With increasing relative humidity the amount of water ($n \sim 1.33$) within the pores of the aluminosilicate thin film increases and displaces nitrogen gas ($n \sim 1.00$); the average refractive index of the thin film increases. This results in the optical mode being increasingly 'pulled' further out of the waveguide and thus the extent of the evanescent wave increases. Therefore more of the optical mode experiences the increasing refractive index of the thin film, which in turn, increases the sensitivity of the mode to further increases in refractive index. Thus the magnitude of the Bragg wavelength shift increases in a quadratic manner as further exemplified in Fig. 1(a). For the case of relative humidity values >60%RH, it is proposed that saturation of the pores had occurred and only multilayers of adsorbed water are forming on the top surface of the thin film. This argument is supported by the work of Al-Abadleh who demonstrated that above 70%RH formation of a liquid-like water layers form on aluminium oxide surfaces [49]; with it known that water is readily adsorbed on aluminium oxide [50]. The larger error bars calculated for the data at the highest %RH values also suggest that multilayers of water are forming; it has been demonstrated previously that uneven coverage of the sensor surface with condensed water leads to increased uncertainty of the Bragg wavelength [25].

Therefore it is proposed that the difference in the humidity response profile is due to a higher rate of water adsorption on the aluminium oxide surface compared to the silica surface. This leads to saturation of the aluminium oxide surface at %RH < 100% whereas the silica thin film is never saturated under the conditions in this experiment. This is corroborated by the heats of adsorption for water on silica and aluminium oxide which are ~59 kJ mol^{-1} [51] and ~70 kJ mol^{-1} [52], respectively; the greater the magnitude of the heat of adsorption the more favoured adsorption becomes and thus the equilibrium is shifted towards adsorption of the water molecules on the surface.

To confirm the long-term operation of this optical hygrometer, its application outside of the flow system was investigated. The Bragg grating hygrometer device was installed in the open laboratory and the Bragg wavelength shift was sampled every 30 s over an eleven hour period whilst the relative humidity recorded from the electronic hygrometer (in close proximity to the Bragg grating hygrometer device) was sampled manually every 30 min. The temperature-compensated response of the Bragg grating device to changes in relative humidity over the course of the day is overlaid in

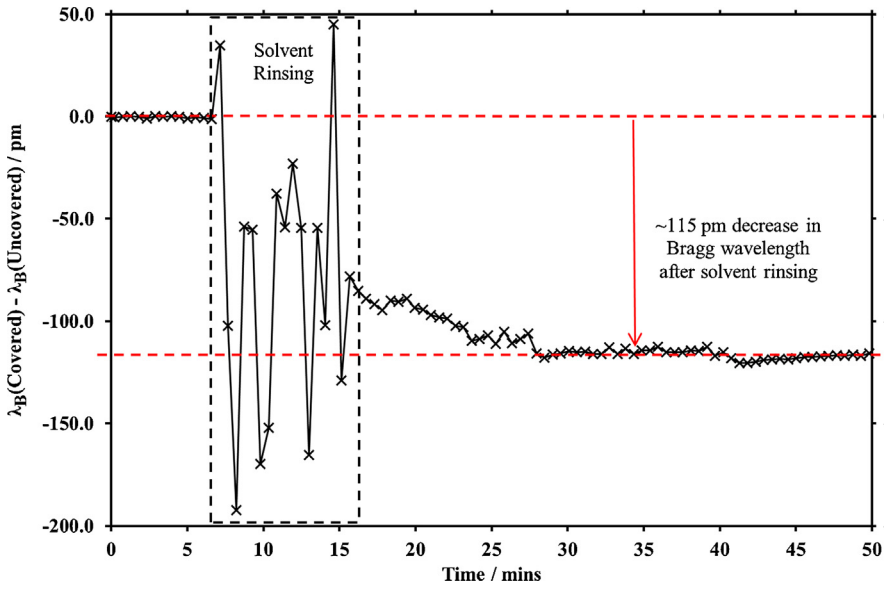

Fig. 7. The decrease in Bragg wavelength upon rinsing the contaminated aluminosilicate thin film Bragg grating hygrometer with methyl ethyl ketone (MEK) indicated the removal of surface contamination. The sharp jumps in refractive index within the hashed region correspond to individual solvent washes.

Fig. 6. It was found that the temperature-referenced Bragg wavelength shifts data was in agreement with the change in %RH as measured by the *Testo 625* hygrometer, within the associated accuracy error of each measurement taken the experimental period. The excellent agreement and lack of long-term drift of the Bragg wavelength shift data demonstrated that the thermal compensation afforded by on-chip reference gratings is a sufficient method to compensate for refractive index changes due to temperature change in 'static' sensing environments as well as 'flow' sensing environments.

4.3. Removal of surface contamination

Over a period of several weeks of regular experimental use, a loss of sensitivity to humidity was noticed with the alumina-grafted optical hygrometer that was not accompanied by the reduction in film thickness which was exhibited by the silica analogue. The cause of this was attributed to grease within the laboratory nitrogen gas lines liberated under high flow.

It was found that full sensitivity to changes in humidity could however be repeatedly and completely restored, by rinsing the planar device with organic solvent. In situ refractive index monitoring during a rinsing cycle of methyl ethyl ketone followed by isopropanol revealed the removal of a contaminant, as shown by the negative Bragg wavelength shift in Fig. 7, plotted after correction against the reference Bragg gratings. It should be noted that whilst the reference returned to its initial value, this was only once all solvent had evaporated and the effects of evaporative cooling diminished, however these effects would be experienced by all gratings equally – further illustrating the need for on-chip compensation. It was found that the alumina-grafted sol–gel layer was resistant to a wide range of organic solvents, including methyl ethyl ketone, isopropanol, methanol, dichloromethane, *n*-hexane, acetone, xylenes and water with no decrease in film thickness being detected after prolonged exposure.

5. Conclusion

We have demonstrated that a planar integrated Bragg grating sensor chip fabricated using the direct UV-writing approach can be modified with a mesoporous silica thin film. Such a device is highly sensitive to changes in humidity over a wide humidity range; however hydrolytic degradation of the sol–gel requires the additional grafting of alumina to the porous surface to ensure long-term stability. Such alumina-grafting offers the additional benefits of enhanced sensitivity, up to 3 times that of the silica analogue, and for applications at elevated humidity. The sensitivity of the aluminium oxide modified thin film device, in the range 0–65%RH, was 0.69 ± 0.05%RH/pm. Compared to photonic crystal fibre-based humidity sensors reported in the literature, the device reported herein is less intrinsically sensitive [10]. However, with further optimisation of the film thickness and enhancement of the evanescent modal overlap we believe that the sensitivity of this first proof-of-concept device technique can be improved. In addition, the device reported herein offers the additional real-world benefits of multiplexed sensing and self-referencing. The device has been shown to be resistant to solvent vapours and solvents, an important factor for real-world applications.

Long-term measurement indicated that the thermal compensation afforded by on-chip reference grating was sufficient to prevent any drift in calibration. As with all hygrometers, contamination of the sensor can occur, for the reported devices this was easily removed by rinsing with organic solvent with the sensitivity being repeatedly and reproducibly restored.

The facile fabrication techniques, robustness, and associated advantages of the planar integrated optical format make this device a viable humidity sensor that offers advantages over the current electrical devices in a range of domestic, commercial and industrial settings. When this is combined with the previously reported methods for monitoring temperature [8], pressure [53], and chemo/bio-detection [18] the suitability of integrated optical Bragg grating devices for highly multiplexed sensor devices within distributed networks becomes apparent.

Acknowledgements

DJW would like to thank the EPSRC (EPSRC DTG: EP/P505119/1) and IS:CE Chem Interreg IVA Programme France (Channel) – England No.# 4061 for funding this work. DJW would also like to thank Prof. Jeremy Frey for a fruitful discussion on the kinetics of adsorption on surfaces.

References

[1] Z. Chen, C. Lu, Sensor Letters 3 (2005) 274–295.
[2] I. Cacciari, G.C. Righini, Optical gas sensing, in: E. Comini, G. Faglia, G. Sberveglieri (Eds.), Solid State Gas Sensing, Springer Science + Business Media, New York, 2009, pp. 209–236.
[3] British Standards Institution, Humidity – Part 1: Terms, Definitions and Formulae, British Standard BS 1339-1 2002, British Standards Institution, London, 2002.
[4] E. Sinha, Meteorological & Geoastrophysics Abstracts 13 (1962) 3622–3717.
[5] T.L. Yeo, T. Sun, K.T.V. Grattan, Sensors and Actuators A 144 (2008) 280–295.
[6] Z.M. Rittersma, Sensors and Actuators A 96 (2002) 196–210.
[7] O.S. Wolfbeis, Analytical Chemistry 76 (2004) 3269–3284.
[8] S. Zheng, Y. Zhu, S. Krishnaswamy, Proceedings of SPIE 7983 (2011) 79831A.
[9] S. Zheng, Y. Zhu, S. Krishnaswamy, Proceedings of SPIE 8346 (2012) 83460D.
[10] S. Zheng, Y. Zhu, S. Krishnaswamy, Sensors and Actuators B 176 (2013) 264–274.
[11] S. Dubinsky, G.S. Grader, G.E. Shter, M.S. Silverstein, Polymer Degradation and Stability 86 (2004) 171–178.
[12] J. Janata, Principles of Chemical Sensors, Springer Science+Business Media, New York, 2009.
[13] R.M. Parker, J.C. Gates, M.C. Grossel, P.G.R. Smith, Sensors and Actuators B 145 (2010) 428–432.
[14] L.A. Coldren, S.W. Corzine, M.L. Masanovic (Eds.), Diode Lasers and Photonic Integrated Circuits, second ed., John Wiley & Sons, New Jersey, 2012.
[15] J. Yoshida, IEEE Transactions on Components, Hybrids and Manufacturing Technology 16 (1993) 778–782.
[16] P.J. Skrdla, S.S. Saavedra, N.R. Armstrong, S.B. Mendes, N. Peyghambarian, Analytical Chemistry 71 (1999) 1332–1337.
[17] G. Schulz-Ekloff, D. Wöhrle, B. van Duffel, R.A. Schoonheydt, Microporous and Mesoporous Materials 51 (2002) 91–138.
[18] B. Bhola, P. Nosovitskiy, H. Mahalingam, W.H. Steier, IEEE Sensors Journal 9 (2009) 740–747.
[19] P. Prosposito, C. Palazzesi, F. Michelotti, V. Fogiletti, M. Casalboni, Journal of Sol–Gel Science and Technology 60 (2011) 395–399.
[20] M. Rosenberger, G. Koller, S. Belle, B. Schmauss, R. Hellmann, Optics Express 20 (2012) 27288–27296.
[21] B.A. Miller-Chou, J.L. Koenig, Progress in Polymer Science 28 (2003) 1223–1270.
[22] R.M. Parker, J.C. Gates, M.C. Grossel, P.G.R. Smith, Applied Physics Letters 95 (2009) 173306.
[23] R.M. Parker, J.C. Gates, D.J. Wales, P.G.R. Smith, M.C. Grossel, Lab Chip 13 (2013) 377–385.
[24] I.J.G. Sparrow, G.D. Emmerson, C.B.E. Gawith, P.G.R. Smith, M. Kaczmarek, A. Dyadyusha, Applied Physics B 81 (2005) 1–4.
[25] M. Olivero, M. Svalgaard, Optics Express 13 (2005) 8390–8399.
[26] D.O. Kundys, J.C. Gates, S. Dasgupta, C.B.E. Gawith, P.G.R. Smith, IEEE Photonics Technology Letters 21 (2009) 947–949.
[27] G.D. Emmerson, S.P. Watts, C.B.E. Gawith, V. Albanis, M. Ibsen, R.B. Williams, P.G.R. Smith, Electronics Letters 38 (2002) 1531–1532.
[28] C.B.E. Gawith, G.D. Emmerson, S.G. McKeekin, J.R. Bonar, R.I. Laming, R.B. Williams, P.G.R. Smith, Electronics Letters 39 (2003) 1050–1051.
[29] I.J.G. Sparrow, P.G.R. Smith, G.D. Emmerson, S.P. Watts, C. Riziotis, Sensors (2009) 607647.
[30] I.J.G. Sparrow, G.D. Emmerson, C.B.E. Gawith, P.G.R. Smith, Sensors and Actuators B 107 (2005) 856–860.
[31] S. Achmann, G. Hagen, J. Kita, I.M. Malkowsky, C. Kiener, R. Moos, Sensors 9 (2009) 1574–1589.
[32] X. Xu, J. Wang, Y. Long, Sensors 6 (2006) 1751–1764.
[33] X. Liu, S. Zheng, X. Zhang, J. Cong, K. Chen, J. Xu, Chinese Optics Letters 2 (2004) 683–685.
[34] P.C.A. Jerónimo, A.N. Araújo, M. Conceicao, B.S.M. Montenegro, Talanta 72 (2007) 13–27.
[35] O. Lev, M. Tsionsky, L. Rabinovich, V. Glezer, S. Sampath, I. Pankratov, J. Gun, Analytical Chemistry 67 (1995) 22A–30A.
[36] A. Abdelghani, J.M. Chovelon, N. Jaffrezic-Renault, M. Lacroix, H. Gagnaire, C. Veillas, B. Berkova, M. Chomat, V. Matejec, Sensors and Actuators B 44 (1997) 495–498.
[37] F. Abdelmalek, J.M. Chovelon, M. Lacroix, N. Jaffrezic-Renault, V. Matejec, Sensors and Actuators B 56 (1999) 234–242.
[38] C.J. Brinker, G.W. Scherer, Sol–Gel Science: The Physics and Chemistry of Sol–Gel Processing, Academic Press, New York, 1990.
[39] E. Stamper, R.L. Koral (Eds.), Handbook of Air Conditioning Heating and Ventilating, third ed., Industrial Press Inc., New York, 1979.
[40] Y. Lu, R. Ganguli, C.A. Drewien, M.T. Anderson, C.J. Brinker, W. Gong, Y. Guo, H. Soyez, B. Dunn, M.H. Huang, J.I. Zink, Nature 389 (1997) 364–368.
[41] S. Tao, G. Li, H. Zhu, Journal of Materials Chemistry 16 (2006) 4521–4528.
[42] D.R. Dunphy, S. Singer, A.W. Cook, B. Smarsly, D.A. Doshi, C.J. Brinker, Langmuir 19 (2003) 10403–10408.
[43] Testo Ltd., Testo 625 – Humidity/Temperature, 2013, http://www.testolimited.com/p/227/testo-625-humiditytemperature (Accessed 20th January 2013).
[44] L. Chia-Yen, L. Gwo-Bin, Sensor Letters 3 (2005) 1–15.
[45] C. McDonagh, F. Sheridan, T. Butler, B.D. MacCraith, Journal of Non-Crystalline Solids 194 (1996) 72–77.
[46] J.M.D. Consul, I.M. Baibich, E.V. Benevenutti, D. Thiele, Química Nova 28 (2005) 393–396.
[47] M.E. Azim-Araghi, A. Krier, Thin film (ClAlPc) phthalocyanine gas sensors, in: S.M. Vaezi-Nejad (Ed.), Selected Topics in Advanced Solid State and Fibre Optic Sensors, The Institute of Engineering and Technology (IET), London, 2000.
[48] G.W.C. Kaye, T.H. Laby, Tables of Physical and Chemical Constants, Longman, London, 1971.
[49] H.A. Al-Abadleh, V.H. Grassian, Langmuir 19 (2003) 341.
[50] J.B. Peri, Journal of Physical Chemistry 69 (1965) 211.
[51] J. Puibasset, R.J.-M. Pellenq, Journal of Chemical Physics 118 (2003) 5613.
[52] Y.I. Tarasevich, I.G. Polyakova, V.E. Polyakova, Theoretical and Experimental Chemistry 36 (2000) 113.
[53] C. Holmes, L.G. Carpenter, J.C. Gates, P.G.R. Smith, Journal of Micromechanics and Microengineering 22 (2012) 025017.

Biographies

Dominic J. Wales is a postgraduate student studying for a PhD in Chemically Functionalised Bragg Grating Gas Sensors collaborating between the ORC and the School of Chemistry at the University of Southampton. He graduated from the University of Southampton with a MChem in Chemistry in 2009.

Richard M. Parker is currently a Research Fellow at the ORC at the University of Southampton. He gained a MChem degree in chemistry from the University of Southampton in 2007. In collaboration with the ORC, his PhD thesis investigated the application of supramolecular and surface chemistry to an integrated optical refractometer for application in chemical sensing. After completion of his PhD studies in 2010, he continued researching in the field of optical sensors and supramolecular chemistry at the University of Southampton.

James C. Gates is currently a Senior Research Fellow at the ORC at the University of Southampton. He gained an MPhys degree from the University of Southampton in 1999, and completed his PhD at the ORC in 2003. His PhD thesis investigated the optical properties of various photonic devices at a nanometre scale using an interferometeric near-field technique. He continued researching in the field of nanophotonics in the Physics Department at the University of Southampton before returning to the ORC in 2006. He is currently developing planar integrated optical devices for a wide range of applications in telecommunications and detection.

Martin C. Grossel is a Reader in Organic Chemistry at the University of Southampton where he has been since 1991 and Organic Chemistry tutor at Christ Church, University of Oxford since 1973. He graduated from King's College, University of London, with a BSc in 1970 and a PhD in Physical Organic Chemistry in 1974. He has published over 90 journal papers together with books, reviews and patents. His research interests have focussed on conformational analysis of small organic molecules, molecular electronics, crystal engineering and applications of photoactive polymers and dendrimers within the fields of biology, optoelectronics and materials science.

Peter G.R. Smith is a Professor in the ORC and the Department of Electronics and Computer Science at the University of Southampton. He graduated from Oxford University with a BA in Physics in 1990 and DPhil in Nonlinear Optics in 1993. After a year spent as a management consultant he joined the University of Southampton. He has worked on a number of areas in optics ranging from laser spectroscopy to polymer integrated optics. He has published over 180 journal and conference papers in the fields of periodically poled materials and UV-written devices, including invited talks at national and international meetings.